AN INVESTIGATION OF THE CONVERGENCE OF WAVE SLAM AVERAGE PEAK ACCELERATIONS FOR SMALL HIGH-SPEED PLANING CRAFT

FINAL

6 February 2021

Prepared By:

The Columbia Group (TCG)
100 M Street SE, Suite 900
Washington, DC 20003

Prepared For:

Naval Surface Warfare Center Carderock Division Detachment Norfolk
1400 Tarawa Court
Bldg 1602, Suite #303
Little Creek – Fort Story Joint Expeditionary Base
Virginia Beach, Virginia 23459-3239

Contract Number #N0017819D7741
Task Instruction TI001

REPORT DOCUMENTATION PAGE

Form Approved
OMB No. 0704-0188

1. REPORT DATE *(DD-MM-YYYY)*	**2. REPORT TYPE**	**3. DATES COVERED** *(From - To)*
6-02-2021	Final	July 2020 to February 2021

An Investigation of the Convergence of Wave Slam Average Peak Accelerations for Small High-Speed Craft

5a. CONTRACT NUMBER

5b. GRANT NUMBER

5c. PROGRAM ELEMENT NUMBER

6. AUTHOR(S)
Michael R. Riley

5d. PROJECT NUMBER

5e. TASK NUMBER

5f. WORK UNIT NUMBER

7. PERFORMING ORGANIZATION NAME(S) AND ADDRESS(ES)

The Columbia Group (TCG)
100 M Street SE, Suite 900
Washington, DC 20003

8. PERFORMING ORGANIZATION REPORT NUMBER

TCG-TI001-1-2021

9. SPONSORING / MONITORING AGENCY NAME(S) AND ADDRESS(ES)
Naval Surface Warfare Center Carderock Division
Detachment Norfolk, Combatant Craft Division
2600 Tarawa Court, Suite #303
Virginia Beach, Virginia 23459-3239

10. SPONSOR/MONITOR'S ACRONYM(S)
NSWCCD Det Norfolk

11. SPONSOR/MONITOR'S REPORT

12. DISTRIBUTION / AVAILABILITY STATEMENT
DISTRIBUTION STATEMENT A. Approved for public release; distribution is unlimited.

13. SUPPLEMENTARY NOTES

14. ABSTRACT Acceleration data is recorded during high-speed craft trials to quantify the severity of wave impacts. The ride severity parameters most often derived from the data have been the average of the largest one percent of all peak accelerations and the average of the largest ten percent of all peaks. The amplitude of the average accelerations has been shown to converge to a relatively stable value as more and more data is recorded. This report summarizes an investigation of the factors that lead to the apparent convergence of the average accelerations.

15. SUBJECT TERMS
Seakeeping peak accelerations wave impact statistics

16. SECURITY CLASSIFICATION OF:			**17. LIMITATION OF ABSTRACT**	**18. NUMBER OF PAGES**	**19a. NAME OF RESPONSIBLE PERSON:** Michael Riley
a. REPORT	**b. ABSTRACT**	**c. THIS PAGE**			**19b. TELEPHONE NUMBER** *(include area code)*
Unclassified	Unclassified	Unclassified	See 12.	32	757-492-4950

Standard Form 298 (Rev. 8-98)
Prescribed by ANSI Std. Z39.18

EXECUTIVE SUMMARY

This report summarizes the results of an investigation of the convergence of average peak accelerations as more and more peaks are recorded during rough-water trials of small high-speed craft. Existing guidance from multiple sources suggest that more peaks is better, but how much more, and what engineering rationale should substantiate the answer? To address the question, simplified equations and numerous examples of peak acceleration data sets are presented.

The approach employed in this investigation was based on disregarding how $A_{1/M}$ statistics have been or are to be applied in the future. The focus was to only consider what the average accelerations and ratios describe, and how the metrics vary as more and more peak accelerations are added to a data set.

The results demonstrate that convergence of the average of the highest 10 percent of peaks ($A_{1/10}$), the average of the highest 1 percent of peaks ($A_{1/100}$), and the $A_{1/100}/A_{1/10}$ ratio means that the shape of the cumulative distribution of the peak acceleration data set becomes more stable as the number of peak acceleration data points increases. A simple percent difference criterion is presented for quantifying the stability of the cumulative distribution shape.

RECOMMENDATION

The data sets presented in this report include various parametric options to illustrate why and how $A_{1/M}$ values vary with increasing N. The options included low, medium, and large A_{max} amplitudes, as well as the occurrence of A_{max} early, in the middle, or late in a run. The options within the seven data sets serve the purpose, but more is better. Additional data sets should be investigated to further demonstrate the convergence and oscillation phenomena.

PUBLIC RELEASE APPROVAL

The contents of this report were approved for Distribution Statement A: approved for public release; distribution is unlimited, by the Congressional and Public Affairs Branch, Naval Surface Warfare Center Carderock Division on 2 September 2020, Request ID #NSWCCD-002647.

TABLE OF CONTENTS

TABLE OF FIGURES

LIST OF TABLES

1 INTRODUCTION

1.1 FABRICATED PEAK ACCELERATIONS

The focus of this report is on the statistical variation of acceleration values rather than the response amplitudes for specific craft. The example data sets presented herein were therefore fabricated from original data sets so that tables and data plots do not represent the impact amplitudes of any specific craft, any specific craft speed, or any specific wave height environment. The peak accelerations extracted from the original time histories were scaled by a constant value, but the sequence in which the peaks occurred in time were maintained. The histograms and cumulative distributions of peak accelerations are, therefore, characteristic of the seaway in which the data were obtained.

1.2 ACCELERATION DATA

Error! Reference source not found. is a relatively short acceleration time history recorded during a seakeeping trial. The red curve is the unfiltered acceleration that includes rigid body and local vibration responses. The black curve is the 10-Hertz (Hz) low-pass filtered acceleration. Each spike, or peak, in the curve is caused by an individual wave impact. Low-pass filtering provides an estimate of the rigid

body acceleration, which is proportional to the force acting on the craft section at the gauge location (Riley, Coats, Murphy, 2014). The low-pass filtered peaks are proportional to the maximum wave impact load in units of "g", the local acceleration of gravity. Figure 2 is a plot of all 151 rigid body peak accelerations derived from the record that are larger than the root-mean-square (RMS) acceleration of the time history. The peaks in Figure 2 and all peak acceleration amplitudes (i.e., rigid body estimates) presented in this report were extracted from acceleration records by *StandardG* software (Riley, Haupt, Jacobson, 2010 and Zseleczky, 2012). In **Error! Reference source not found.**, the peaks are plotted largest-to-smallest from left to right. The maximum peak acceleration (A_{max}) is 5.31 g.

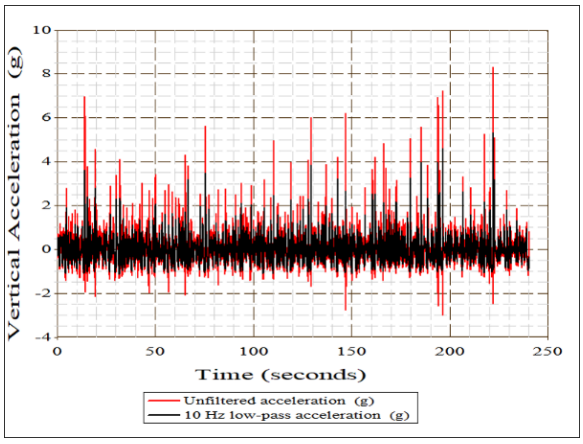

Figure 1. Example Vertical Acceleration Data

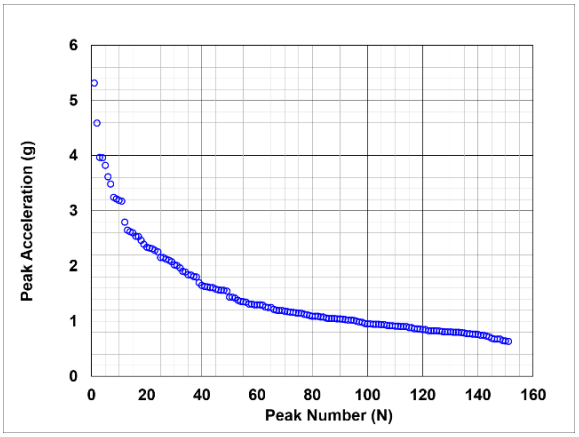

Figure 2. Rigid Body Peak Accelerations

1.3 AVERAGE ACCELERATIONS

In addition to the maximum peak acceleration value (A_{max}), many trial reports tabulate four additional statistics to characterize the data set, including the RMS acceleration of the entire time history record, the average of the highest 33 percent of peaks accelerations ($A_{1/3}$), the average of the highest 10 percent of peaks ($A_{1/10}$), and the average of the highest 1 percent of peaks ($A_{1/100}$). The general form of the equation for computing the average accelerations is given by equation **Error! Reference source not found.**.

$$A_{1/M} = \frac{\sum_1^{N/M} a_i}{N/M} \quad (1)$$

N is the number of peak accelerations in the data set, and a_i are the peak accelerations sorted largest to smallest , with i = 1 being the largest peak acceleration (A_{max}). Typically, M is 3, 10, or 100 for the three average values. The absolute value of the ratio N/M is applied. For example in **Error! Reference source not found.**, N = 151 peak acceleration values are plotted largest-to-smallest. $A_{1/10}$ is, therefore, the average of the 15 highest values (151/10) equal to 4.19g. $A_{1/3}$ is the average of the 50 highest values (151/3) equal to 2.41 g. The RMS acceleration of the time history is 0.63 g.

1.4 HOW MANY PEAKS?

A consistent *StandardG* process has proven to be useful. It provides unambiguous comparisons of estimated rigid body accelerations over a broad range of organizations and practitioners, but it does not address how many peaks (N) should be recorded during a trial. The question is often expanded to include how many peaks are needed for the calculated results to be statistically significant, or to ensure a high confidence level in the processed data.

The International Towing Tank Conference (ITTC) provides ranges of suggested N values for seakeeping experiments. For irregular waves, N = 50 should be taken as a lower limit, larger values are preferred, and N = 100 is more usual as the standard, but N = 200 or above is considered excellent practice (ITTC, 2011a). For experiments involving rarely occurring events these values are increased to N = 100, 200, and 400 (ITTC, 2011b). STANAG 4154 (2000) indicates full-scale seakeeping trials should have no less than 100 wave encounters for a wide variety of ship types, but primarily for displacement monohull and SWATH (small water-plane area twin hull) ships (STANAG 4154, 2000).

Researchers have also combined computer simulations with scale-model data to introduce the concept of $A_{1/M}$ statistical convergence. Significantly more than 100 peaks are required for convergence (Rosen and Garme, 2004), (Razola, Rosen, Garme, 2014). In a later publication, the results of numerous tank runs and longer duration computer simulations indicated N = 500 was appropriate for $A_{1/100}$ convergence (Rosen, Begovic, Razola, Garme, 2017).

While consistency is limited among these references, many conclude that more is better. But how much more, and what engineering rationale substantiates the answer? These questions will be pursued, but first two approaches related to more-is-better will be discussed.

1.5 RECORD STACKING

Combining data from multiple runs is a widely accepted practice, when processing acceleration data recorded during scale-model trials (Fridsma, 1971), (Zarnick and Turner, 1981), (Rosen, Begovic, Razola, Garme, 2017). For similar wave spectrum conditions, the results of multiple short duration tow-tank runs are combined (or stacked) to create a longer data record that has more peak accelerations than the individual short-duration runs.

However, another form of record stacking is not recommended. When acceleration data have been recorded during a run, the acceleration record for the single run can be added to itself multiple times to provide a longer duration run, and, therefore, many more peak accelerations. For example, if a 15-minute acceleration record were stacked onto itself to achieve a total 30-minute run time, the resulting stacked record will have twice the number of peak accelerations. Equation **Error! Reference source not found.**, however, demonstrates that a problem exists with this approach. Let the integer S be the number of times a record is stacked onto itself. From equation **Error! Reference source not found.**, when the integer S is substituted into equation **Error! Reference source not found.**, it appears in the

numerator and denominator and cancels out, which yields a trivial result. The $A_{1/M}$ values for the S stacked records are the same as the $A_{1/M}$ values for the original unstacked record.

$$A_{1/M}^{Stacked} = \frac{\sum_1^{SN} a_i}{SN/M} = \frac{S\sum_1^{N} a_i}{S\ N/M} = A_{1/M} \tag{2}$$

Stacking a record onto itself S times to achieve an increase in the number of peaks (N) is not recommended.

1.6 CUMULATIVE BINOMIAL DISTRIBUTION

Another approach to be avoided is the use of the cumulative binomial distribution in an attempt to answer the how-many-peaks question in terms of statistical significance, confidence level, or data reliability. **Error! Reference source not found.** is a probability nomogram applicable to binary testing, which has only two possible outcomes (e.g., pass or fail) (STAT T&E COE, 2013). The axis on the right, with a scale from 0.001 to 0.999, should be labelled the probability (P) of c or fewer occurrences in N trials (e.g., c = 3 failures). The axis on the left, with a scale from 0.50 to 0.99, should be labelled the probability (p) of occurrence (i.e., failure) in a single trial (STAT T&E COE, 2013). In the figure, the axis on the right is often mislabeled confidence level, and the axis on the left is mislabeled reliability (STAT T&E COE, 2013).

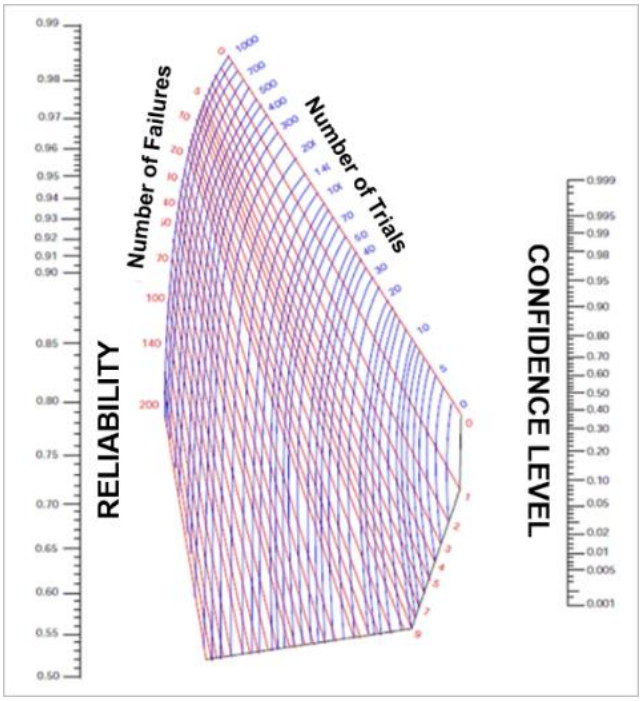

Figure 3. Probability Nomograph, STAT T&E COE (2013)

Trials of small high-speed craft in waves, on full-scale or model-scale, are not binary trials with only two outcomes. Therefore, words like confidence level, reliability, or inferred statistical significance

should not be applied when analyzing peak accelerations. Other statistics, including $A_{1/M}$ values, root-mean-square, standard deviations, confidence interval, and max/min values are appropriate.

1.7 APPROACH

As an important first step, the approach taken in this investigation is to disregard how the $A_{1/M}$ statistics have been or are to be used, as in (Koelbel, 2000), (Koelbel, 2001), or (ABS HSNC, 2007). The focus is rather on analyzing $A_{1/M}$ variations as more and more peak accelerations are added to data.

2 ACCELERATION STATISTICS

2.1 NOMOGRAPH BEGINNINGS

Error! Reference source not found. is the nomogram published by Fridsma in his seminal report that introduced the concept of applying probability distributions to peak acceleration responses for small craft in irregular waves (Fridsma, 1971). The axis on the right is the percentage of acceleration values that are less than or equal to a peak value. The outer most axis on the left is the percentage of acceleration values that are greater than a peak value. The inboard axis on the left is the number (N) of peak accelerations. At the time before the wide spread use of computers, the nomograph format provided a very convenient tool for plotting parametric variations for a given mathematical relationship. But, even more convenient is the equation shown in **Error! Reference source not found.** and repeated here in ratio format as equation **Error! Reference source not found.** (i.e., with revised notation compatible throughout this report).

$$A_{1/M}/A_{average} = (1 + lnM) \tag{3}$$

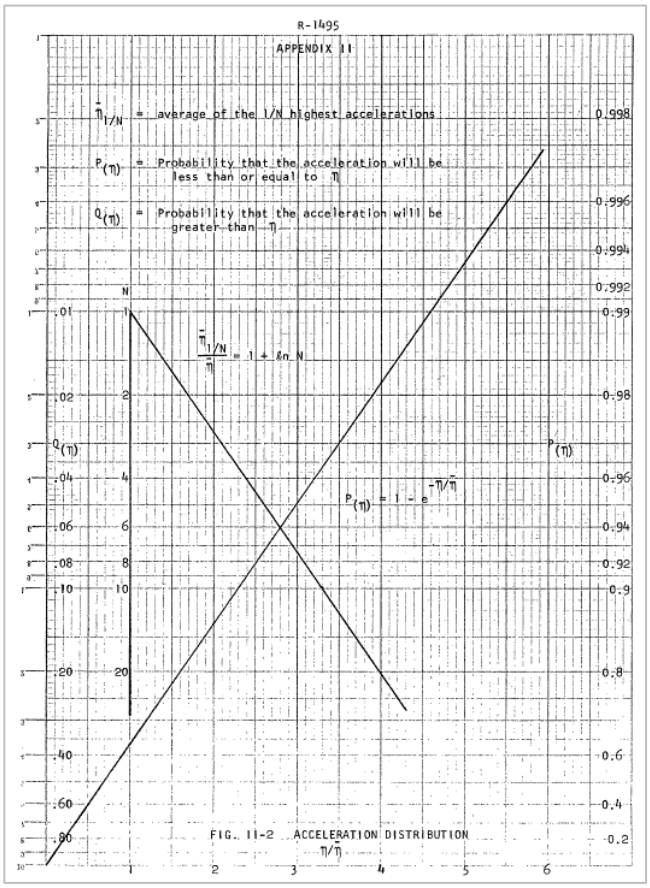

Figure 4. Distribution by Fridsma (1971)

The term $A_{average}$ in equation (3) is the average of all peak accelerations. This equation was applicable because the cumulative distribution curve for the data was reported to exhibit the shape that one would expect from an exponentially distributed population. For the exponential distribution, the ratio of $A_{1/10}$ to $A_{average}$ is 3.30. Likewise, the ratio of $A_{1/100}$ to $A_{average}$ is 5.60, and the ratio of $A_{1/100}$ to $A_{1/10}$ is 1.69. These ratios and equation (3) uniquely characterize the shape of the exponential distribution curve.

Error! Reference source not found. is an example cumulative distribution curve for N = 1768 peak acceleration values recorded during a full-scale rough-water trial. The red bars illustrate the range of peak acceleration values for calculation of the $A_{1/100}$, $A_{1/10}$, $A_{1/3}$, and A_{avg} values. The ratio of any of the $A_{1/M}$ averages is very convenient measure because it uniquely identifies the shape of the cumulative distribution curve. For example, the $A_{1/100}$ to $A_{1/10}$ ratio is 1.31 for a Raleigh cumulative distribution. For a log-normal cumulative distribution it is 1.77. Therefore, in the simplest terms, the $A_{1/100}/A_{1/10}$ ratio and the $A_{1/M}$ values for a set of N peak accelerations are convenient statistics that characterize the shape of the population's cumulative distribution curve.

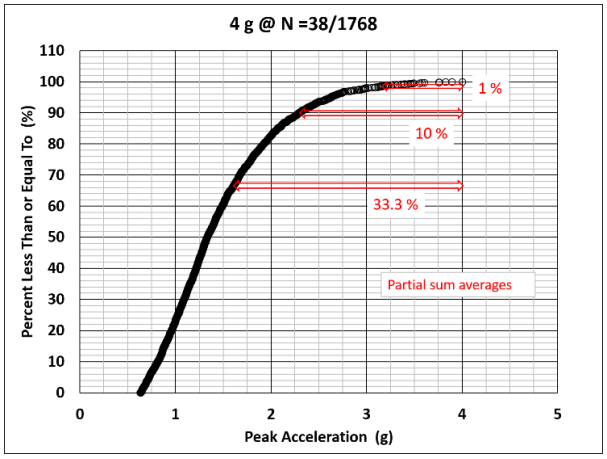

Figure 5. Example Cumulative Distribution Curve

2.2 ANALYSIS PROCESS

The following example illustrates the process to investigate how $A_{1/M}$ values vary as more and more peak accelerations are recorded. The process was applied to recorded full-scale data as well as simplified equations to better understand the parameters that affect $A_{1/M}$ variation with increasing N.

Figure 6 shows the population of peak vertical accelerations for the cumulative distribution curve in **Error! Reference source not found.**. The acceleration time history was processed by the *StandardG* algorithm (with 20 Hz low-pass Kaiser filter) to estimate the peak rigid body accelerations caused by individual wave impacts. The abscissa is the peak number, N, and the ordinate is peak acceleration in units of g. One-thousand-seven-hundred sixty-eight peak accelerations with amplitudes greater than the root-mean-square (RMS) of the time history were recorded during the 30-minute run.

The red arrows in **Error! Reference source not found.** illustrate the sequential process applied during the investigation. The top arrow indicates $A_{1/M}$ statistics were computed with the first N = 100 peak accelerations. The next lower arrow indicates $A_{1/M}$ statistics were computed with the first N = 200 peaks, then the first N = 300 peaks, and until calculations were made for N = 1768. Each set of data for N = 100, 200, 300, 400, 500, etc., is referred to herein as a data subset. The maximum peak acceleration is 4.0 g. Its location in the data set is at N = 38 (i.e., early in the record among the first 100 peaks). The notation for all examples in the report will follow this format: A_{max} = 4.0 g at N = 38/1768 (i.e., 38th peak of 1768 peaks).

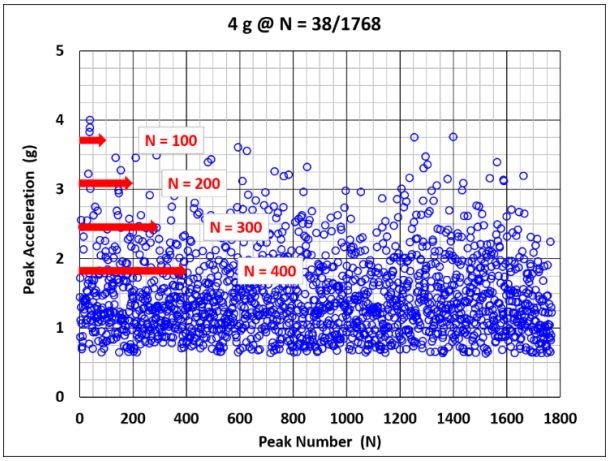

Figure 6. Example Peak Acceleration Data Set

2.3 EXAMPLE 1: A_{MAX} = 4 G AT N = 38/1768

The calculated $A_{1/M}$ values are listed in **Error! Reference source not found.** for the data set in **Error! Reference source not found.**, as well as the $A_{1/100}/A_{1/10}$ ratios. The histograms of data subsets are in **Error! Reference source not found.**. The abscissa is the number of peak accelerations, and the ordinate is peak acceleration in 0.1-g bins. The plot shows that the shape of the curves increase to the right, as more and more groups of 100 peaks are added to the subsets, with eighty percent of the peak amplitudes in the 0.5 g to 2.0 g range.

The tail distribution (i.e., the percentage of values greater than or equal to) for the data subsets is in **Error! Reference source not found.**. This is a useful format because it shows all the data points for computation of $A_{1/100}$ to the left of 0.1 %. Likewise, peaks for computation of $A_{1/10}$ are to the left of 1 %, and peaks for $A_{1/3}$ are to the left of 33.3 % (Riley, Haupt, Ganey, 2015). The abscissa is the logarithm of the percentage of peaks that are greater than or equal to a peak value, and the ordinate is peak acceleration. The plots show that as N increases the curves shift to the left with no increase in peak amplitude because A_{max} occurred early in the record. The cumulative distribution curve for all N = 1768 peaks is shown in **Error! Reference source not found.**.

Table 1. $A_{1/M}$ Values A_{max} = 4 g at N = 38/1768

N	Acceleration Statistics			
	A1/100	A1/10	A1/3	A 1/100 / A 1/10
100	4.000	3.113	2.269	1.285
200	3.946	2.950	2.197	1.337
300	3.906	2.911	2.210	1.342
400	3.824	2.796	2.151	1.368
500	3.758	2.804	2.146	1.340
600	3.733	2.776	2.134	1.344
700	3.707	2.800	2.157	1.324
800	3.676	2.801	2.168	1.312
900	3.651	2.789	2.173	1.309
1000	3.630	2.764	2.156	1.313
1100	3.608	2.731	2.136	1.321
1200	3.584	2.712	2.127	1.321
1300	3.609	2.745	2.150	1.315
1400	3.620	2.763	2.162	1.310
1500	3.602	2.754	2.161	1.308
1600	3.589	2.756	2.169	1.302
1700	3.574	2.743	2.159	1.303
1768	3.574	2.728	2.145	1.310

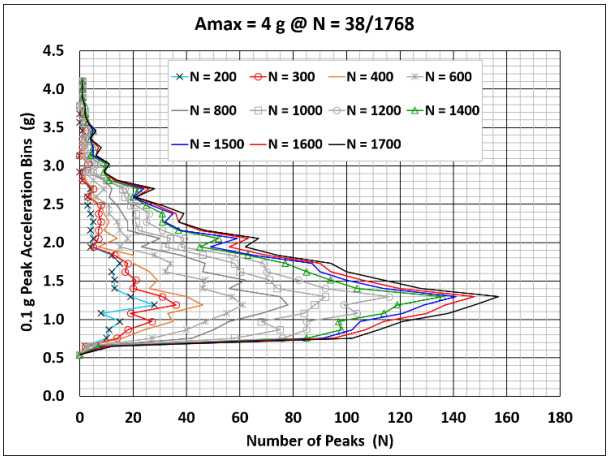

Figure 7. Histogram for A_{max} = 4 g at N = 38/1768

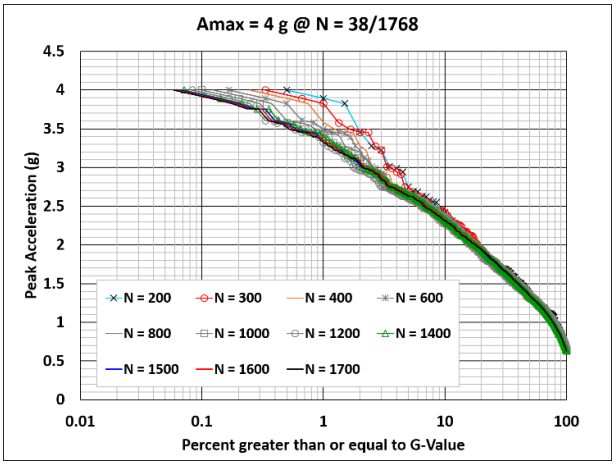

Figure 8. Example Tail Distribution

The cumulative distribution curves are illustrated in **Error! Reference source not found.** above the 90-percent level for the histograms shown in **Error! Reference source not found.**. The peak acceleration variation is on the order of 0.1 g to 0.4 g for percentiles above 90 percent.

A plot of $A_{1/100}$, $A_{1/10}$, $A_{1/3}$ and the $A_{1/100}$ to $A_{1/10}$ ratio for the different data subsets is in **Error! Reference source not found.**. The solid red circle is the location of A_{max} = 4.0 g. The curves appear to converge to a relatively constant value as N increases. $A_{1/3}$ appears to converge first at about N = 200, followed by $A_{1/10}$ at N = 400 and $A_{1/100}$ at N = 1200. The $A_{1/100}$ to $A_{1/10}$ ratio varies from 1.28 to 1.37, indicating the cumulative distribution shape varies roughly ±4.5 % from the shape of a Raleigh distribution ($A_{1/100}/A_{1/10}$ = 1.31).

The different histograms and distributions in Figures 7, 8, and 9 demonstrate that each data subset has a unique histogram and a unique distribution shape. Therefore, the $A_{1/M}$ values and the $A_{1/100}$ to $A_{1/10}$ ratios listed in **Error! Reference source not found.** are unique values for each data subset. With each successive addition of 100 peak accelerations, the sample changes to a new unique subset. But what about the change in the values and the appearance of convergence over time? To address this question, the next section introduces two simple parameters.

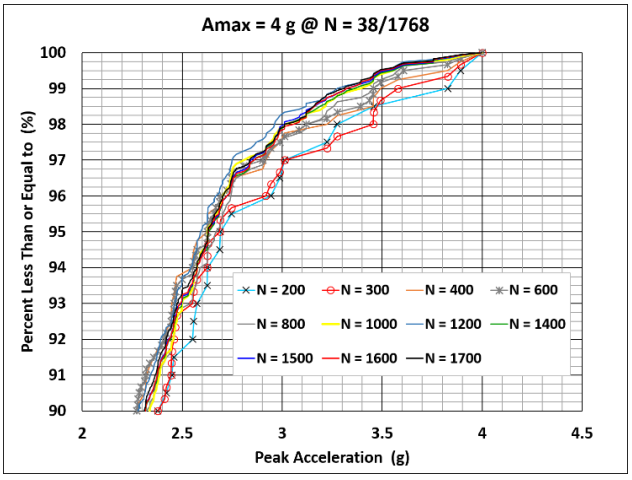

Figure 9. Cumulative Distributions for A_{max} = 4 g

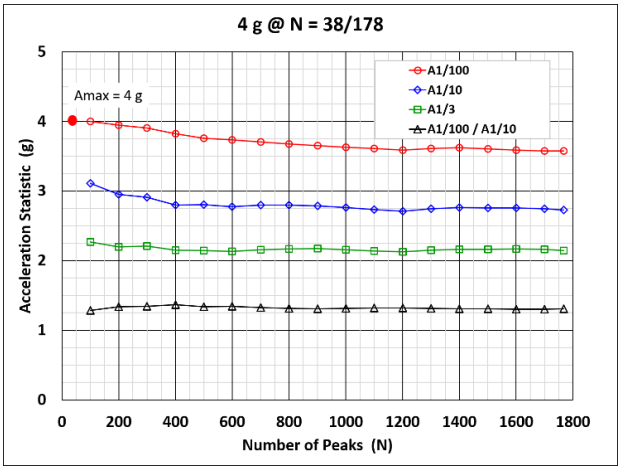

Figure 10. Variation of Statistics with Increasing N

3 THE SUMMATION EQUATION

Equation **Error! Reference source not found.** for $M = 100$ can be rewritten in a different format to show the relationship between computed $A_{1/100}$ values for successive subsets of $N = 100$ additional peaks.

Let $X = |N/100|$ for $X > 1$ (e.g., $[X, N] = [5, 500]$), and define a_i as the ith peak acceleration in the list of peaks (sorted largest to smallest). The notation a_i represents the subset of peak accelerations sorted largest to smallest for $i = 1$ to X.

$$A^{X}_{1/100} = \frac{X-1}{X}\left(A^{X-1}_{1/100}\right) + \frac{a_X}{X} \tag{4}$$

The notation $A^{X}_{1/100}$ is introduced to indicate the number of peaks for computation of the $A_{1/100}$ value. For example for $X = 5$ (for $N = 500$), the highest 5 peaks in the subset are a_1 through a_5. Substitution into equation **Error! Reference source not found.** yields:

$$A^{5}_{1/100} = \frac{4}{5}\left(A^{4}_{1/100}\right) + \frac{a_5}{5} \tag{5}$$

$A^{5}_{1/100}$ indicates the $A_{1/100}$ value is computed with $N = 500$ peaks ($X = 5$), and $A^{4}_{1/100}$ denotes the $A_{1/100}$ value is computed from $N = 400$ ($X = 4$). When $X = 1$ (i.e., N=100), $A^{1}_{1/100} = a_1$.

Table 2 lists the sorted peaks from $N = 100$ to $N = 900$ for the peak accelerations shown in Figure 6. The $A_{1/100}$ values from **Error! Reference source not found.** are listed at the bottom of each column.

Table 2. Highest Sorted Peak Accelerations

N	a(i)	Sorted Peak Accelerations (g)								
100	a1	4.0000	4.0000	4.0000	4.0000	4.0000	4.0000	4.0000	4.0000	4.0000
200	a2		3.8919	3.8919	3.8919	3.8919	3.8919	3.8919	3.8919	3.8919
300	a3			3.8270	3.8270	3.8270	3.8270	3.8270	3.8270	3.8270
400	a4				3.5786	3.5786	3.6065	3.6065	3.6065	3.6065
500	a5					3.4918	3.5786	3.5786	3.5786	3.5786
600	a6						3.4918	3.5535	3.5535	3.5535
700	a7							3.4918	3.4918	3.4918
800	a8								3.4574	3.4574
900	a9									3.4551
A1/100		4.0000	3.9459	3.9063	3.8244	3.7579	3.7326	3.7070	3.6758	3.6513

Equation **Error! Reference source not found.** will now be rewritten in a format that has two new variables related to the differences between peaks and $A_{1/100}$ values. The purpose of the variables is to gain insight into the nature of the variation of $A_{1/M}$ values as more and more peak accelerations (i.e., sets of 100 peaks) are added to the population. The two simple parameters are the population density ratio (ρ) and the difference function delta (δ).

3.1 PEAK ACCELERATION DENSITY RATIO

The peak acceleration density ratio (ρ) is given by equation **Error! Reference source not found.**.

$$\rho = \frac{a_{X+1}}{a_X} \tag{6}$$

It is a measure of how close the peak accelerations are spaced in the list of sorted peaks. As an example, **Error! Reference source not found.** lists the sorted peak accelerations from **Error! Reference source not found.**. The computed values of ρ are tabulated in the last column. The values from 0.9424 to 0.9993 indicate closely spaced values.

Table 3. Sorted Peaks and Density Ratios

N	a(i)	Sorted Peaks	a (i+1) / a(i)
100	a1	4.0000	*
200	a2	3.8919	0.9730
300	a3	3.8270	0.9833
400	a4	3.6065	0.9424
500	a5	3.5786	0.9923
600	a6	3.5535	0.9930
700	a7	3.4918	0.9827
800	a8	3.4574	0.9901
900	a9	3.4551	0.9993
1000	a10	3.4352	0.9942

3.2 $A_{1/100}$ DIFFERENCE FUNCTION

The difference function (δ) is given by:

$$\delta = A_{1/100}^{X+1} - A_{1/100}^{X} \tag{7}$$

Error! Reference source not found. lists the $A_{1/100}$ values from **Error! Reference source not found.**, and the difference between successive values of $A_{1/100}$ as N increases from N = 100 to N = 900. The subscript 1/100 has been omitted for each letter "A" in the column labelled "Equation".

Table 4. Example Values of Delta

N	A1/100 (g)	A1/100 Difference	
		Equation	Value (g)
100	4	*	*
200	3.9459	A^2-A^1	-0.0541
300	3.9063	A^3-A^2	-0.0396
400	3.8244	A^4-A^3	-0.0819
500	3.7579	A^5-A^4	-0.0665
600	3.7326	A^6-A^5	-0.0252
700	3.7070	A^7-A^6	-0.0256
800	3.6758	A^8-A^7	-0.0312
900	3.6513	A^9-A^8	-0.0245
1000	3.6297	A^{10}-A^9	-0.0216
1100	3.6082	A^{11}-A^{10}	-0.0215
1200	3.5843	A^{12}-A^{11}	-0.0239
1300	3.6091	A^{13}-A^{12}	0.0248
1400	3.6197	A^{14}-A^{13}	0.0106
1500	3.6023	A^{15}-A^{14}	-0.0173
1600	3.5894	A^{16}-A^{15}	-0.0130
1700	3.5736	A^{17}-A^{16}	-0.0157

3.3 SIMPLIFYING ASSUMPTIONS

Two simplifying assumptions will now be pursued to better understand how population density affects calculated $A^X_{1/100}$ values and δ values as N increases. First, the maximum peak acceleration ($A_{\max}$) in a recorded acceleration time history occurs within the first 100 peak accelerations (i.e., early in time). The second assumption is that the density function (ρ) in a hypothetical list of sorted peak accelerations is constant. In other words:

$$a_2 = \rho a_1 = \rho A_{\max}$$

$$a_3 = \rho a_2 = \rho^2 A_{\max}$$

$$a_4 = \rho^3 A_{\max}, \text{ and so on.}$$

For constant ρ when $a_1 = A_{max}$, and $X > 1$, equation **Error! Reference source not found.** can be rewritten as:

$$A^X_{1/100} = \frac{A_{max}}{X}(1 + \rho + \cdots \rho^{X-1}) \tag{8}$$

Substitution of equation **Error! Reference source not found.** into equation **Error! Reference source not found.** yields the non-dimensional difference equation as a function of ρ.

$$\frac{\delta^X}{A_{max}} = \frac{1}{X}\left\{1 + \sum_1^{X-1} \rho^i\right\} - \frac{1}{X-1}\left\{1 + \sum_1^{X-2} \rho^i\right\} \tag{9}$$

When $X = 2$, the last summation on the right is zero.

A plot of equation **Error! Reference source not found.** is shown in **Error! Reference source not found.**. The abscissa is X (i.e., N/100) and the ordinate is the non-dimensional δ. The different curves are for values of constant ρ that vary from 0.7 to 0.995. The curves show that for lower density ratios (e.g., $\rho = 0.7$) the non-dimensional form of delta ($\delta/A_{\max}$) is larger than for population densities with

larger values of ρ. When $\rho > 0.97$, the curves are essentially flat with increasing X because the mathematical differences from equation **Error! Reference source not found.** are in the 3rd decimal place. Equation **Error! Reference source not found.** is useful because it helps understand $A^X_{1/100}$ variation as X increases (for the assumed conditions). This is illustrated further in **Error! Reference source not found.** where the $A_{1/100}$ values from **Error! Reference source not found.** are compared with the hypothetical constant ρ curves from **Error! Reference source not found.**.

The black curve with open circles in **Error! Reference source not found.** shows how computed $A_{1/100}$ varies as more data is added to the population over time. The maximum peak acceleration is 4.0 g occurring at N = 37 of 1768 peaks. The straight line curves were computed with equation **Error! Reference source not found.** assuming constant ρ values of 0.97, 0.98, and 0.99. The curves show that the recorded data (black curve) follows the constant ρ = 0.97 curve for roughly the first 500 peaks, then it tends to follow the slope of the ρ = 0.99 curve until roughly N = 1200. Beyond N = 1200, it exhibits small oscillations on the order of 0.03 g.

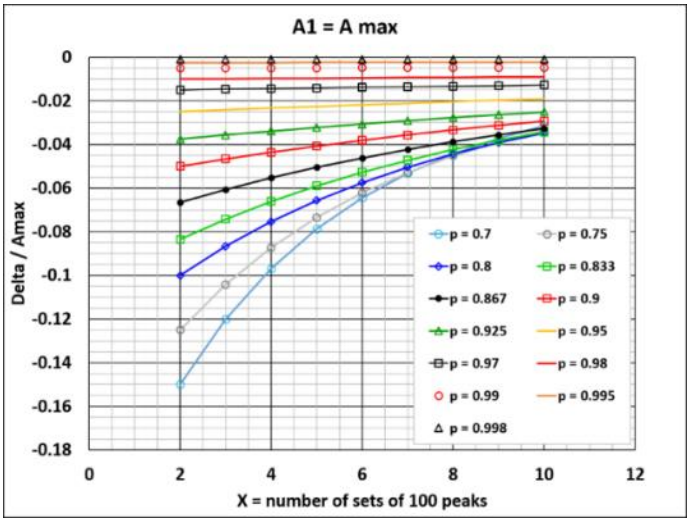

Figure 11. Non-dimensional Difference Equation

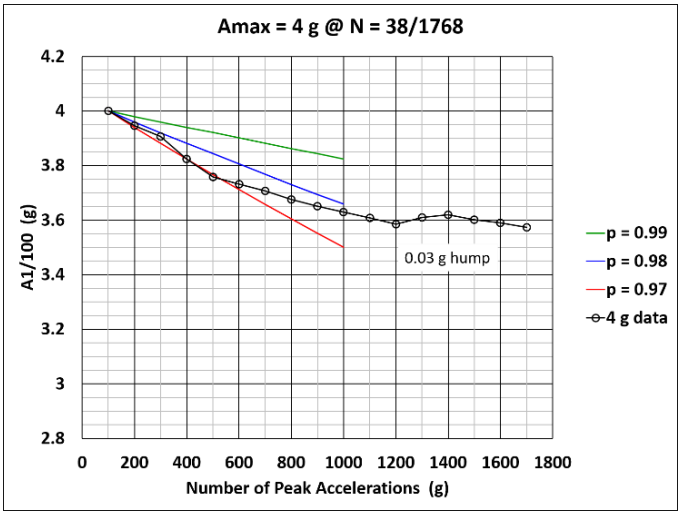

Figure 12. Variation with Increasing Population Density

The small oscillation in **Error! Reference source not found.** after N = 1200 is caused by the occurrence of two roughly 3.75 g peak accelerations. The peaks are observed in **Error! Reference source not found.** between N = 1200 and N = 1400. In equation **Error! Reference source not found.** format, the 13th and 14th values of $A_{1/100}$ (i.e., N = 1300 and N = 1400) in equation **Error! Reference source not found.** are larger than the 12th value of $A_{1/100}$ because a_{13} and a_{14} are larger than the previous a_4 to a_{12} values:

$$A_{1/100}^{14} = \frac{13}{14}\left(A_{1/100}^{13}\right) + \frac{a_{14}}{14} \tag{10}$$

3.4 CONVERGENCE AND OSCILLATION

Figures 10 and 12 clearly show the appearance of converging $A_{1/M}$ curves with later oscillations that are explained with the help of **Error! Reference source not found.** and equation **Error! Reference source not found.**. Lower population densities (e.g., 0.7) result in larger δ values relative to A_{max}. Larger densities (e.g., 0.95) caused by increasing N result in smaller δ values. In addition, the amplitude of δ is directly proportional to A_{max}. The oscillations in the curves as N increases are caused by ± values of δ introduced by higher and lower peak accelerations encountered in the acceleration time history. The oscillation amplitudes decrease over time due to the increasing density ratio.

Given that $A_{1/100}$, $A_{1/10,}$ and $A_{1/100}/A_{1/10}$ are metrics that characterize the cumulative distribution shape, the appearance of convergence implies that the shape of the cumulative distribution is approaching a more stable shape over time. In other words, as more and more peak accelerations are added to the population, the shape of the distribution undergoes smaller and smaller changes due to the preponderance of data already in the population. Each data subset is unique. As more data is added, less difference occurs in distribution shape from the shape of the previous subset distribution.

A useful term for comparing data subsets is the percent difference between each subset value of $A_{1/100}$ and the last calculated value in the data set.

$$A_{1/100}^{X}\ percent\ difference = (100)\frac{A_{1/100}^{X} - A_{1/100}^{Last}}{A_{1/100}^{Last}} \quad (11)$$

The superscript *Last* indicates the last value of $A_{1/100}$ in the data set. **Error! Reference source not found.** lists calculated percent difference values for the $A_{1/100}$ values plotted in **Error! Reference source not found.**. The *Last* value in the table for N = 1768 is 3.574. Thus, the percent difference between N = 100 and N = 1768 is 11.9 %, and so on. Percent difference values for the $A_{1/100}$ to $A_{1/10}$ ratio are also tabulated. The table shows that the percent difference of each value relative to the last value decreases rapidly as N increases.

Table 5. Percent Difference Values

N	A1/100	% Diff from end	A 1/100 / A 1/10	% Diff from end
100	4.000	11.932	1.285	-1.914
200	3.946	10.419	1.337	2.089
300	3.906	9.310	1.342	2.444
400	3.824	7.017	1.368	4.415
500	3.758	5.156	1.340	2.291
600	3.733	4.450	1.344	2.624
700	3.707	3.734	1.324	1.064
800	3.676	2.860	1.312	0.184
900	3.651	2.174	1.309	-0.063
1000	3.630	1.569	1.313	0.253
1100	3.608	0.968	1.321	0.843
1200	3.584	0.300	1.321	0.870
1300	3.609	0.993	1.315	0.352
1400	3.620	1.289	1.310	0.012
1500	3.602	0.804	1.308	-0.163
1600	3.589	0.441	1.302	-0.586
1700	3.574	0.000	1.303	-0.544
1768	3.574	0.000	1.310	0.000

4 A_{MAX} LOCATION, AMPLITUDE, AND DENSITY

Six additional data sets and percent difference plots are presented in the following paragraphs. The data sets were selected to demonstrate the effects of A_{max} location in time (early, middle, and late in the record), A_{max} amplitude, and population density (ρ).

4.1 EXAMPLE 2: 4 G AT N = 1209/1768

Error! Reference source not found. shows an example data set, where the maximum peak acceleration is 4 g occurring relatively late in time at N = 1209 of 1768. A_{max} and two other large peak accelerations occur before N = 1400. **Error! Reference source not found.** shows how the calculated $A_{1/M}$ changes with increasing N. $A_{1/100}$ values initially increase, then level-off and decrease again until A_{max} is encountered.

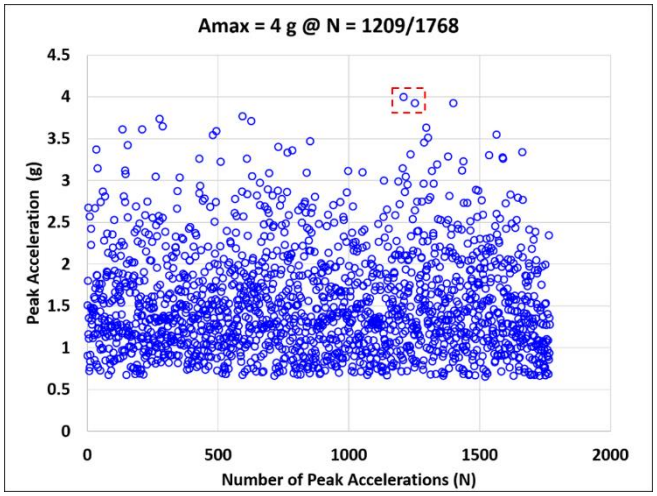

Figure 13. A_{max} = 4 g Later at N = 1209/1768

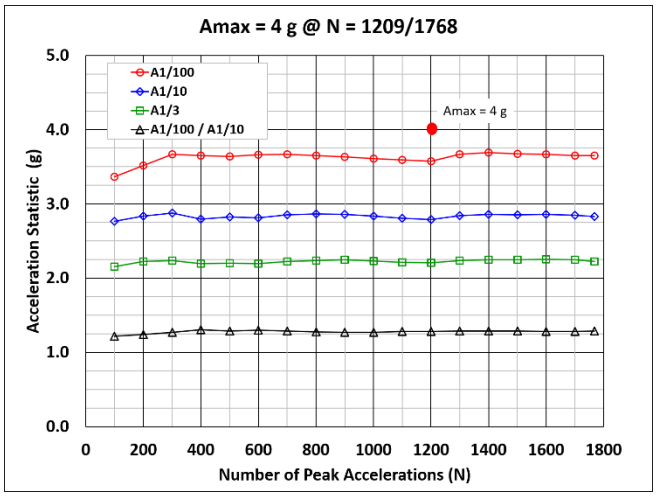

Figure 14. Variation of Statistics for A_{max} = 4 g N = 1209

4.2 EXAMPLE 3 & 4: 10 G AT N = 89/535 AND 324/533

Error! Reference source not found. shows a different peak acceleration data set where A_{max} is 10 g at N = 89 of 535 peaks (i.e., occurring early in time). Figure 16 shows how the variation of $A_{1/M}$ would have been different if A_{max} had occurred later at N = 324 of 535 peaks. For these calculations the first 300 peaks where arbitrarily shifted manually to the end of the original record. The curves show that when A_{max} is early the $A_{1/100}$ values decrease with increasing N. When A_{max} occurs later in time, the $A_{1/100}$ values increase with increasing N until A_{max} is encountered. The tabulated $A_{1/M}$ values and percent differences are provided in APPENDIX A. The convergence of $A_{1/100}/A_{1/10}$ to 1.93 is a higher ratio than a log-normal distribution (ratio = 1.77). In Figure 16, the apparent convergence yields an $A_{1/100}$ value 17.5 % less the A_{max} value.

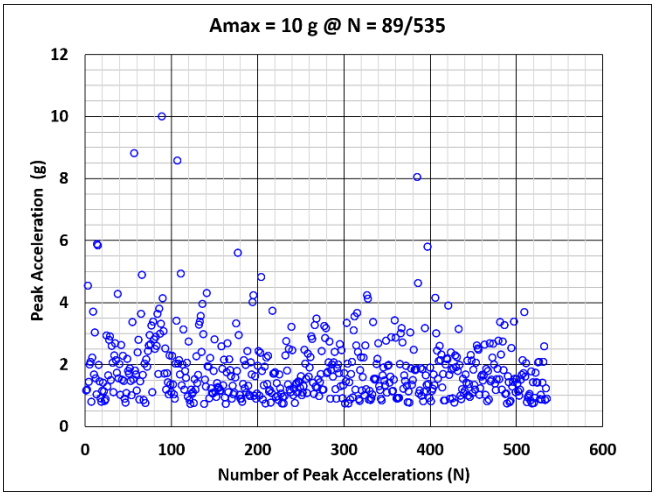

Figure 15. A_{max} = 10 g Early N < 100

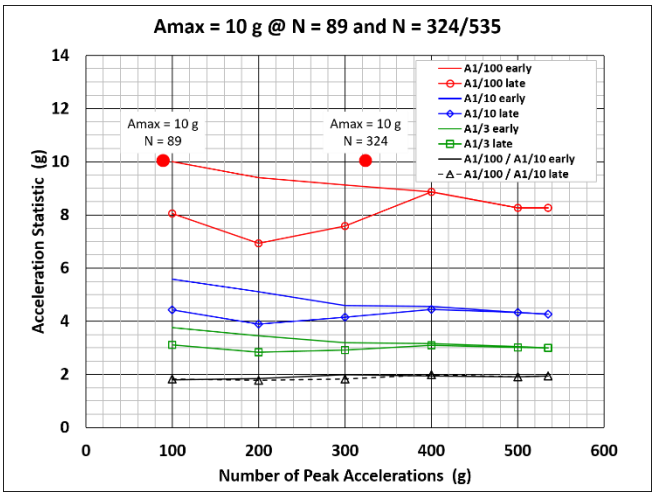

Figure 16. Variation of Statistics for A_{max} = 10 g

4.3 EXAMPLE 5: 15.0 G AT N = 601/1106

Error! Reference source not found. shows an example of acceleration peaks with a larger A_{max} = 15.0 g occurring near the middle of a record at N = 601/1106. **Error! Reference source not found.** shows the corresponding variation of $A_{1/M}$ values. All of the $A_{1/100}$ values are 21 % to 33 % less than the A_{max} value. The tabulated $A_{1/M}$ values and percent differences are provided in APPENDIX A. The convergence of $A_{1/100}/A_{1/10}$ to 1.47 is a ratio between a Raleigh distribution (1.31) and an exponential distribution (1.69).

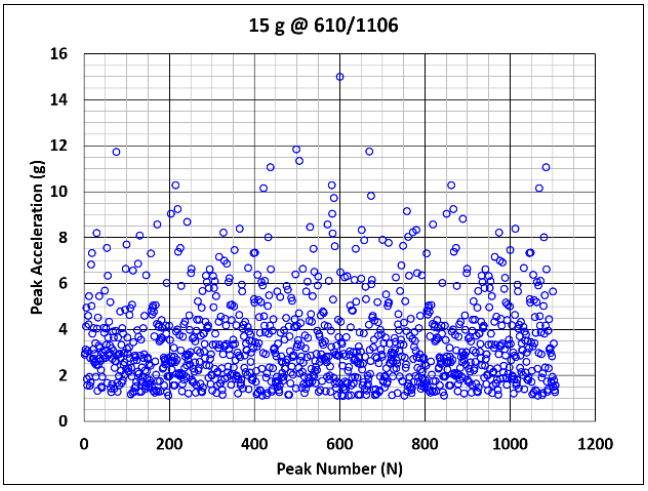

Figure 17. A_{max} = 15 g at N = 601/1106

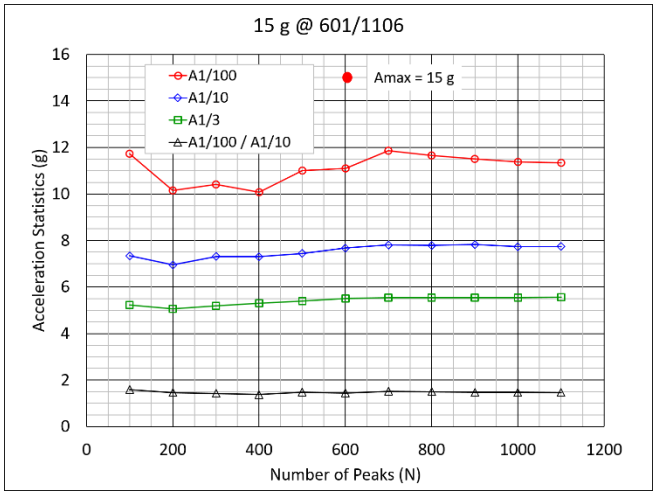

Figure 18. Variation of Statistics for A_{max} = 15 g

4.4 EXAMPLE 6: 12 G AT N = 583/1064

Error! Reference source not found. shows an example of acceleration peaks with A_{max} = 12 g occurring near the middle of a record at N = 583/1064. **Error! Reference source not found.** shows the corresponding variation of $A_{1/M}$ values with increasing N. The $A_{1/100}$ values are 23 % to 36 % less than the A_{max} value. The tabulated $A_{1/M}$ values and percent differences are provided in APPENDIX A.

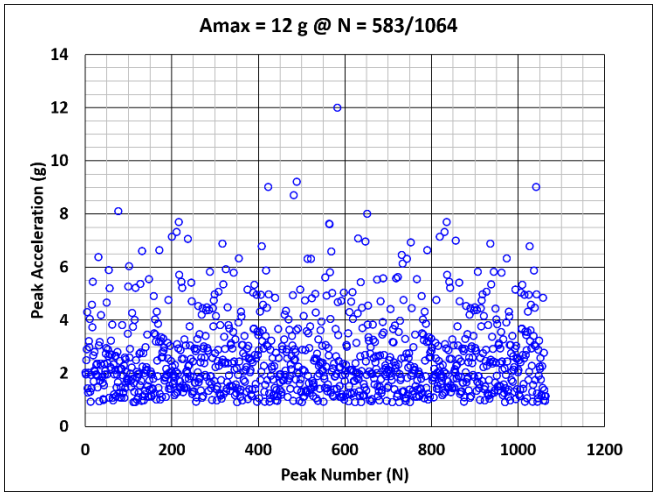

Figure 19. A_{max} = 12 g at N = 583/1064

In Figure 20 the convergence of $A_{1/100}/A_{1/10}$ to 1.44 is a ratio between a Raleigh distribution (1.31) and an exponential distribution (1.69).

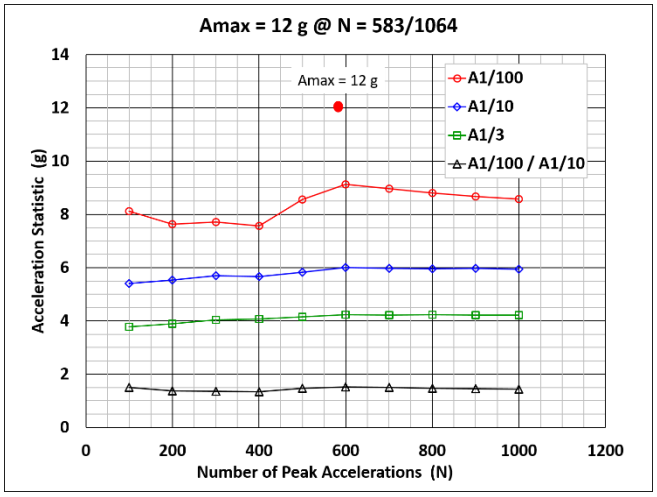

Figure 20. Variation of Statistics for A_{max} = 12 g

4.4 EXAMPLE 7: 7 G AT N = 525/947

Error! Reference source not found. shows an example of acceleration peaks with A_{max} = 7 g occurring near the middle of a record at N = 525/947. The corresponding variation of $A_{1/M}$ values with increasing N is in **Error! Reference source not found.**. All of the $A_{1/100}$ values are 20 % to 30 % less than the A_{max} value. The tabulated $A_{1/M}$ values and percent differences are provided in APPENDIX A. The convergence of $A_{1/100}/A_{1/10}$ to roughly 1.64 is a ratio close to an exponential distribution (1.69).

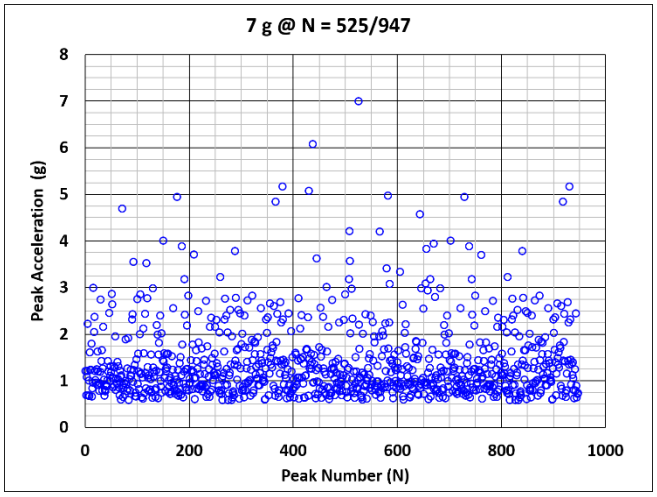

Figure 21. A_{max} = 7 g at N = 525/947

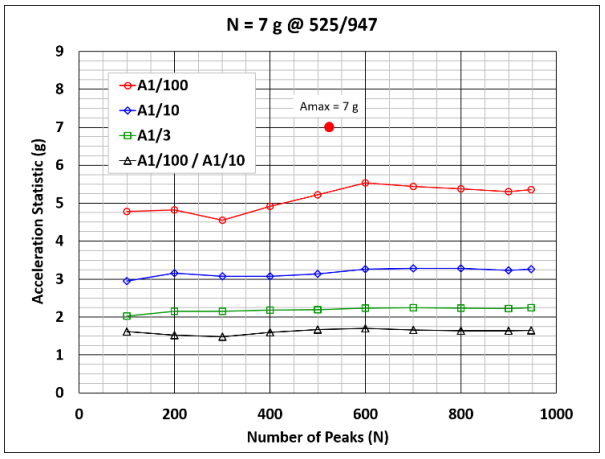

Figure 22. Variation of Statistics for A_{max} = 7 g

5 PERCENT DIFFERENCE PLOTS

5.1 $A_{1/100}/A_{1/10}$ VARIATIONS

The $A_{1/100}/A_{1/10}$ ratio percent difference plots are created in **Error! Reference source not found.** for the seven data sets from equation **Error! Reference source not found.**. The curves clearly show the apparent convergence for different population properties, including large, medium, and small values of A_{max}, and for A_{max} occurring early, middle, or late in time.

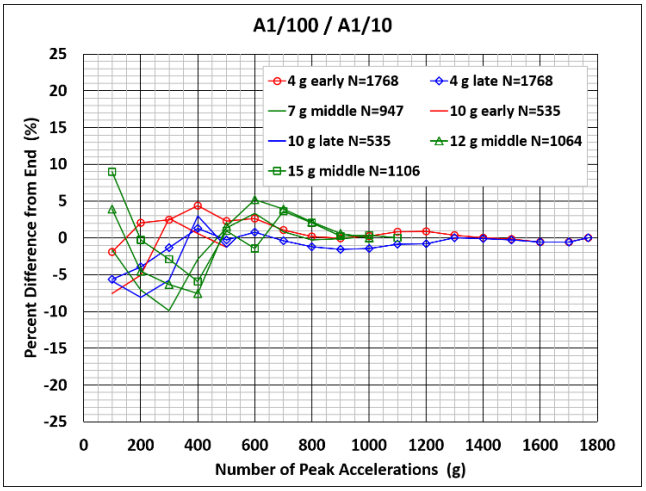

Figure 23. Percent Difference Plots for $A_{1/100}/A_{1/10}$

5.2 $A_{1/100}$ VARIATIONS

The percent difference plots for $A_{1/100}$ values are shown in **Error! Reference source not found.**. The same general trends are observed with increasing N. The values vary within ±20 % for $0 < N < 300$, ±10 % for $N > 400$, ±5 % for $N > 500$, and ±2.5 % for $N > 800$.

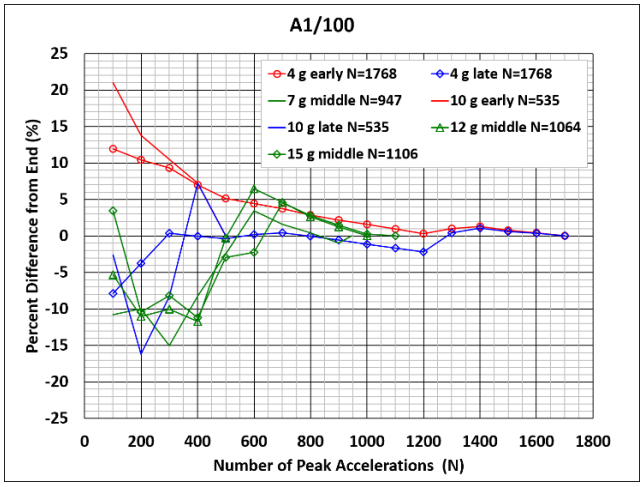

Figure 24. Percent Difference Plots for $A_{1/100}$

6 OBSERVATIONS

6.1 DISTRIBUTION SHAPE CONVERGENCE

The $A_{1/100}/A_{1/10}$ ratios in **Error! Reference source not found.**, which are a measure of the shape of the cumulative distribution plots, vary within ±10 % for $N < 400$, ±5 % for $N < 700$, ±2 % for $N > 800$, ±1 % for $N > 1200$, and ±0.5 % for $N > 1600$. As N increases, the population density increases, which leads to smaller δ values. The distribution shape changes less as N increases. In other words, the distribution shape becomes more stable with increasing N.

The convergence of $A_{1/100}$ values in **Error! Reference source not found.** has the same implications. As N increases, the population density (ρ) increases, which causes smaller and smaller values of δ, which results in smaller and smaller ± changes in $A_{1/100}$. The $A_{1/100}$ values vary within ±20 % for $N < 300$, ±15 % for $N < 400$, ±5 % for $N > 500$, ±2 % for $N > 800$, ±1 % for $N > 1300$, and ±0.5 % for $N > 1600$.

The relative stability of the cumulative distribution shape improves as the percent difference decreases from ±10 %, to ±5 %, to ±2 %, to ±1 %, to ±0.5 %, etc. The percent difference parameter (from the end), therefore, provides a useful criterion for assessing the degree of relative stability in the distribution shape.

6.2 AMAX LOCATION

In **Error! Reference source not found.**, the two red curves for A_{max} early in time show that the $A_{1/100}$ values decrease with increasing N until small oscillations occur as predicted by equation **Error! Reference source not found.**. The curves for A_{max} late in the record (blue) and at the middle of the record (green) tend to increase with increasing N before converging.

6.3 VARIATIONS WITH AMAX AMPLITUDE

Equation **Error! Reference source not found.** for constant ρ shows that the value of δ increases for increasing values of A_{max} if A_{max} occurs when $N < 100$. **Error! Reference source not found.** illustrates the same general trend by comparing the $A_{1/100}$ value at the end of each run with the run A_{max} value. The blue dotted line has a slope of 1.0. From the plot, converged $A_{1/100}$ values are less than A_{max} values (i.e., below the dotted line) by amounts that tend to increase in amplitude with increasing A_{max}. The red dotted line (a least squares fit through the red data points) indicates $A_{1/100}$ values trend an average 23.7 % less than the A_{max} values.

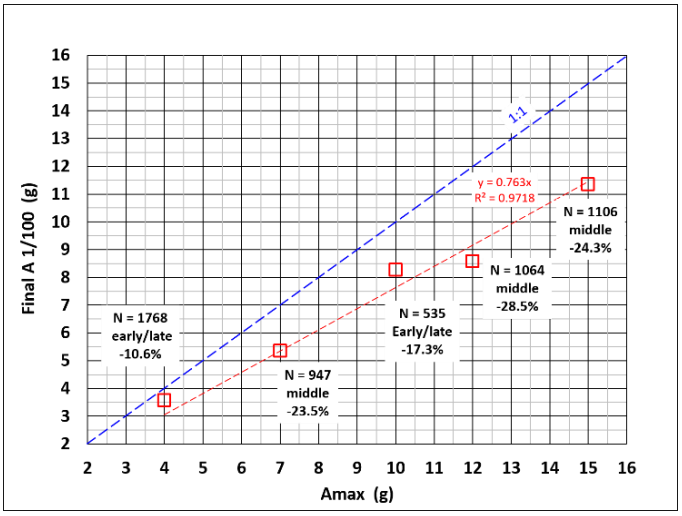

Figure 25. Converged $A_{1/100}$ Values Less Than A_{max}

6.4 A1/10 CONVERGENCE

All the data plots for the first seven examples presented herein show that $A_{1/10}$ values converge sooner than the $A_{1/100}$ values. For each set of N peak accelerations, 10 times more peaks are applied in the $A_{1/10}$ calculation than in the $A_{1/100}$ calculation.

6.5 UNCERTAINTY

An unpublished investigation of available acceleration data indicates the uncertainty in estimating rigid body peak accelerations is less than ± 0.10 percent if: (1) the data processing protocol uses the same type of low-pass filter, the same filter software, and the same cut-off frequency, (2) a minimum 16-bit analogue to digital converter is used, and (3) 25 g piezo-resistive accelerometers are employed.

6.6 THE BENEFIT OF LARGE N

Equations **Error! Reference source not found.** through **Error! Reference source not found.** provide insights into why a large population size (N) is better than a smaller population size (i.e., more is better). As N increases, population density (ρ) increases, the difference between successive $A_{1/100}$ values (δ) decreases, and the $A_{1/100}$ values tend to converge with eventual small oscillations. The shape of the cumulative distribution curve is becoming more and more stable, with smaller and smaller changes in shape as more peaks are added to the population. This leads to a new question. When are smaller and smaller changes in the cumulative distribution shape desirable?

A plausible answer is related to test data comparisons with computer simulations. Time history comparisons of recorded acceleration data with computer simulation results are not feasible because of the wave spectra implementation to characterize the simulation's wave environment. The only viable comparison approach is to compare statistical characteristics of inputs and responses for the recorded data and the simulation (Rosen, Begovic, Razola, Garme, 2017). For example, comparisons of the cumulative distributions of peak accelerations for the recorded data and the simulations could be compared. Similar distribution shapes and amplitudes would be an indication of good correlation. In this approach, to demonstrate that the cumulative distributions had reached a relatively stable shape before attempting the correlation is more important.

6.7 RUN TIME

The concept of a relatively stable distribution shape is observed in the percent difference plots in **Error! Reference source not found.** and **Error! Reference source not found.**. For example, a relatively stable $A_{1/100}/A_{1/10}$ ratio or $A_{1/100}$ value is indicated by the oscillation in the results that are within ±5 %, ±2 %, or ±1 %. The percent difference value can be included with the significant wave height and planned average speed of the craft to estimate the run time duration required to achieve a number N of peak accelerations. This is especially important for test planners who must balance numerous competing factors that determine the run time for scale-model tests as well as full-scale at-sea trials. The relative stability goal related to the percent difference oscillation should be established based on the trial objectives.

6.8 APPROPRIATE QUESTIONS

The previous discussion on the benefits of large N and distribution shape stability suggests that the question, "H*ow many peaks are required for $A_{1/M}$ calculations?"* by itself is too vague to lead to a rationale answer. The question lacks specificity. Given that $A_{1/100}$ and the $A_{1/100}/A_{1/10}$ ratio are metrics that characterize the shape of the population's cumulative distribution curve, other more appropriate questions should be considered.

1. How many peak accelerations are needed to achieve a relatively stable cumulative distribution shape?
2. What is the characteristic shape (e.g., exponential, Raleigh, etc.) of the cumulative distribution curve for a given population of peak accelerations?

3. What run time is required to obtain a sufficient population of peak accelerations to achieve relative stability (e.g., ±1 %, ±2 %, ±5 % parameter change) in the cumulative distribution shape parameter?

6.9 RECOMMENDATION

The data sets presented in this report include various parametric options to illustrate why and how $A_{1/M}$ values vary with increasing N. The options included low, medium, and large A_{max} amplitudes, as well as the occurrence of A_{max} early, in the middle, or late in a run. The options within the seven data sets presented herein serve the purpose, but more is better. Additional data sets should be investigated to further demonstrate the convergence and oscillation phenomena.

7 SUMMARY AND CONCLUSIONS

The approach employed in this investigation was based on disregarding how $A_{1/M}$ statistics have been or are to be applied in the future. The focus was to only consider what the average accelerations and ratios describe, and how the metrics vary as more and more peak accelerations are added to a data set.

In simple statistical terms the results indicate that the $A_{1/100}/A_{1/10}$ ratio and the $A_{1/M}$ values are convenient metrics that uniquely characterize the shape of a population's cumulative distribution curve. Successive subsets of peak acceleration data with increasing population size (N) are all unique, with unique $A_{1/M}$ statistics for each subset. Adding additional peak accelerations to a subset results in a new unique data subset with unique statistics. As N increases, the population density (ρ) increases. The increasing density causes the differences (δ) between successive values of $A_{1/M}$ to decrease. The decreasing δ values manifests itself as convergence in the $A_{1/M}$ versus N curve. Successive additions of larger and smaller peak accelerations in late time is observed as smaller and smaller oscillations in the $A_{1/M}$ versus N curve.

Convergence means the shape of the cumulative distribution of data subsets is changing less and less as N increases. In other words, the population distribution is becoming more stable with increasing N. Where a stable distribution is desirable, one application is comparing statistical distributions between recorded data and computer simulations (Rosen et al., 2017).

When combined with other population statistics, the $A_{1/M}$ values characterize the variation of wave impact amplitudes recorded over time. The values capture how ride severity varied during a run from the most severe wave impact load (A_{max}) to the preponderance of lower amplitude values. What remains now is the application of cogent rationale for applying the $A_{1/M}$ values to practical engineering applications (Riley, Coats, 2012). Caution is advised, however, to avoid the use of binomial theory terms when characterizing a set of peak accelerations (e.g., statistical significance, reliability, or confidence level). Additional data sets should be investigated to further demonstrate the convergence and oscillation phenomena.

8 ACKNOWLEDGEMENTS

The author would like to thank Jason Marshall, Dr. Evan Lee, Heidi Murphy, Brock Aron, and Carl Casamassina from the Combatant Craft Division of Naval Surface Warfare Center Carderock, and Dr. Joel Park, Naval Surface Warfare Center Carderock. Their shared information and review comments significantly improved the quality of the report.

9 REFERENCES

ABS HSNC (2007). "Guide for Building and Classing High Speed Naval Craft, Part 3, Hull Construction and Equipment" Chapter 2-2, para. 1.1.3," American Bureau of Shipping, Houston, TX.

Fridsma, G., (1971). "A systematic Study of the Rough-Water Performance of Planing Boats (Irregular waves – Part II)," Stevens Institute of Technology Report SIT-DL-71-1495.

ITTC (2011a). "Seakeeping Experiments," International Towing Tank Conference Recommended Procedures and Guidelines 7.5-02-07-02.1 Revision 06, September 2017.

ITTC (2011b). "Experiments on Rarely Occurring Events," International Towing Tank Conference Recommended Procedures and Guidelines 7.5-02-07-02.3, Revision 05, September 2017.

Koelbel, Jr., J. G., (2000). "Structural design for High-Speed Craft Part I," *Professional Boatbuilder*, Number 67, pages 31 – 47, October/November 2000.

Koelbel, Jr., J. G., (2001). "Structural design for High-Speed Craft Part II," *Professional Boatbuilder*, Number 68, pages 32 – 43, December/January 2001.

Razola, M., Rosen, A., Garme, K. (2014). "Allen and Jones Revisited," *Ocean Engineering*, 89 (2014) p. 119 – 133.

Riley, M. R., Haupt, K. D., Jacobson, D. R. (2010). "A Generalized Approach and Interim Criteria for Computing $A_{1/N}$ Accelerations Using Full-Scale High Speed Craft Data," Naval Surface Warfare Center Carderock Division Report NSWCCD-23-TM-2010/13, April 2010.

Riley, M. R., Coats, T. W. (2012). "Development of a Method for Computing Wave-Impact Equivalent Static Accelerations for Use in Planing Craft Hull Design," Third Chesapeake Powerboat Symposium, Annapolis, MD, 15-16 June 2012.

Riley, M. R., Coats, T. W., Murphy, H. P., (2014). "Response Mode Decomposition for Quantifying Wave Impact Load in High-Speed Planing Craft," Naval Surface Warfare Center Carderock Division Report NSWCCD-80-TR-2014/007, April 2014.

Riley, M. R., Haupt, K. D., Ganey, H., (2015). "Ride Severity Profile for Evaluating Craft Motions," Naval Surface Warfare Center Carderock Division Report NSWCCD-80-TR-2015/002, May 2015.

Rosen, A., Garme, K. (2004). "Model Experiment Addressing the Impact Pressure Distribution on Planing Craft in Waves," *International Journal of Small Craft Technology*, Volume 146.

Rosen, A., Begovic, E., Razola, M., Garme, K. (2017). "High-speed craft dynamics in waves: challenges and opportunities related to the current safety philosophy," *Proceedings of the 16th International Ship Stability Workshop*, 5 – 7 June 2017, Belgrade, Serbia.

STANAG 4154 (2000). "Common Procedures for Seakeeping in the Ship Design Process," Military Agency for Standardization, Standardization Agreement 4154 (Edition 3), North Atlantic Treaty Organization, Brussels, Belgium, December 2000.

STAT T&E COE (2013). "Use of the Binomial Nomograph for T&E Planning Best Practices," Air Force Institute of Technology, Report STAT T&E COE Report-05-2013, Wright-Patterson Air Force Base, OH, www.AFIT.edu/STAT

Zarnick, E., Turner, C. (1981). "Rough Water Performance of High Length to Beam Ratio Planing Boats," David W. Taylor Naval Ship Research and Development Center Report DTNSRDC/SPD-0973-01, February 1981.

Zseleczky, John (2012). "Behind the Scenes of Peak Acceleration Measurements," The Third Chesapeake Powerboat Symposium, Annapolis, Maryland, USA.

10 APPENDIX A

Table A1 lists values of $A_{1/M}$ and the $A_{1/100}$ to $A_{1/10}$ ratio for A_{MAX} = 4 g occurring relatively late in time at N = 1209 of 1768. Table A2 lists the percent difference values.

Table A1. Statistics for A_{MAX} = 4 g at N = 1209/1768

N	A1/100 (g)	A1/10 (g)	A1/3 (g)	A 1/100 / A 1/10
100	3.366	2.764	2.153	1.218
200	3.517	2.836	2.225	1.240
300	3.666	2.878	2.238	1.274
400	3.652	2.793	2.194	1.308
500	3.640	2.827	2.200	1.287
600	3.661	2.815	2.194	1.300
700	3.668	2.853	2.223	1.286
800	3.653	2.864	2.239	1.276
900	3.633	2.859	2.247	1.271
1000	3.612	2.838	2.232	1.273
1100	3.593	2.807	2.213	1.280
1200	3.574	2.791	2.205	1.280
1300	3.669	2.842	2.236	1.291
1400	3.691	2.862	2.249	1.290
1500	3.676	2.855	2.248	1.288
1600	3.668	2.858	2.257	1.283
1700	3.653	2.845	2.248	1.284
1768	3.653	2.830	2.223	1.291

Table A2. Percent Differences for A_{MAX} = 4 g at N = 1209

N	A1/100	% Diff from end	A 1/100 / A 1/10	% Diff from end
100	3.366	-7.865	1.218	-5.647
200	3.517	-3.723	1.240	-3.933
300	3.666	0.361	1.274	-1.321
400	3.652	-0.026	1.308	1.308
500	3.640	-0.372	1.287	-0.274
600	3.661	0.213	1.300	0.754
700	3.668	0.415	1.286	-0.372
800	3.653	-0.007	1.276	-1.177
900	3.633	-0.562	1.271	-1.562
1000	3.612	-1.138	1.273	-1.405
1100	3.593	-1.656	1.280	-0.848
1200	3.574	-2.168	1.280	-0.802
1300	3.669	0.439	1.291	0.040
1400	3.691	1.050	1.290	-0.070
1500	3.676	0.616	1.288	-0.249
1600	3.668	0.395	1.283	-0.581
1700	3.653	0.000	1.284	-0.533
1768	3.653	0.000	1.291	0.000

Table A3 lists values of $A_{1/M}$ and the $A_{1/100}$ to $A_{1/10}$ ratio for A_{MAX} = 10 g occurring early in time at N = 89 of 535. Table A4 lists values of $A_{1/M}$ and the $A_{1/100}$ to $A_{1/10}$ ratio for A_{MAX} = 10 g occurring later in time at N = 324 of 535. Table A5 lists the percent difference values for earlier and later times for A_{MAX} = 10 g.

Table A 3. Statistics for A_{MAX} = 10 g at N = 89/535

N	Acceleration Statistics			
	A 1/100 (g)	A 1/10 (g)	A 1/3 (g)	A1/100 / A1/10
100	10.000	5.590	3.759	1.789
200	9.407	5.120	3.449	1.837
300	9.131	4.597	3.186	1.987
400	8.862	4.553	3.168	1.946
500	8.266	4.328	3.051	1.910
535	8.266	4.272	3.001	1.935

Table A4. Statistics for A_{MAX} = 10 g at N = 324/535

N	Acceleration Statistics			
	A 1/100 (g)	A 1/10 (g)	A 1/3 (g)	A1/100 / A1/10
100	8.052	4.421	3.107	1.821
200	6.930	3.897	2.844	1.778
300	7.583	4.158	2.914	1.824
400	8.862	4.448	3.099	1.992
500	8.266	4.328	3.014	1.910
535	8.266	4.272	3.001	1.935

Table A5. Percent Difference for A_{MAX} = 10 g

N	10 g Percent Difference					
	A1/100		A1/10		A1/100 / A1/10	
	Later	Earlier	Later	Earlier	Later	Earlier
100	-2.59	20.98	3.49	30.85	-5.88	-7.55
200	-16.16	13.80	-8.78	19.83	-8.09	-5.04
300	-8.26	10.47	-2.67	7.60	-5.74	2.67
400	7.20	7.20	4.11	6.57	2.97	0.59
500	0	0	1.30	1.30	-1.28	-1.28
535	0	0	0	0	0	0

Table A6 lists values of $A_{1/M}$ and the $A_{1/100}$ to $A_{1/10}$ ratio for A_{MAX} = 15 g at N = 601/1106. Table A7 lists the percent difference values.

Table A6. Statistics for A_{MAX} = 15 g

N	Acceleration Statistics			
	A1/100	A1/10	A1/3	A1/100 / A1/10
100	11.735	7.345	5.225	1.598
200	10.159	6.949	5.060	1.462
300	10.417	7.316	5.192	1.424
400	10.072	7.301	5.298	1.380
500	11.013	7.441	5.405	1.480
600	11.090	7.675	5.501	1.445
700	11.860	7.803	5.553	1.520
800	11.662	7.792	5.545	1.497
900	11.508	7.829	5.544	1.470
1000	11.373	7.730	5.540	1.471
1100	11.344	7.737	5.562	1.466

Table A7. Percent Differences for A_{MAX} = 15 g

N	A1/100	% Diff from end value	A1/100 / A1/10	% Diff from end value
100	11.735	3.450	1.598	8.976
200	10.159	-10.449	1.462	-0.290
300	10.417	-8.169	1.424	-2.880
400	10.072	-11.216	1.380	-5.910
500	11.013	-2.915	1.480	0.946
600	11.090	-2.241	1.445	-1.447
700	11.860	4.544	1.520	3.658
800	11.662	2.803	1.497	2.081
900	11.508	1.449	1.470	0.258
1000	11.373	0.255	1.471	0.347
1100	11.344	0.000	1.466	0.000

Table A8 lists values of $A_{1/M}$ and the $A_{1/100}$ to $A_{1/10}$ ratio for A_{MAX} = 12 g at N = 583/1064. Table A9 lists the percent difference values.

Table A8. Statistics for A_{MAX} = 12 g

N	Acceleration Statistics			
	A1/100 (g)	A1/10 (g)	A1/3 (g)	A1/100 / A1/10
100	8.112	5.405	3.773	1.501
200	7.629	5.534	3.890	1.379
300	7.710	5.698	4.033	1.353
400	7.569	5.669	4.070	1.335
500	8.551	5.827	4.149	1.467
600	9.126	6.007	4.237	1.519
700	8.966	5.974	4.224	1.501
800	8.799	5.964	4.227	1.475
900	8.677	5.973	4.219	1.453
1000	8.571	5.935	4.220	1.444

Table A9. Percent Differences for A_{MAX} = 12 g

N	A1/100 (g)	% Diff from end	A1/100 / A1/10	% Diff from end
100	8.112	-5.349	1.501	3.925
200	7.629	-10.993	1.379	-4.543
300	7.710	-10.045	1.353	-6.310
400	7.569	-11.693	1.335	-7.558
500	8.551	-0.237	1.467	1.603
600	9.126	6.471	1.519	5.190
700	8.966	4.612	1.501	3.923
800	8.799	2.663	1.475	2.168
900	8.677	1.236	1.453	0.595
1000	8.571	0.000	1.444	0.000

Table A10 lists values of $A_{1/M}$ and the $A_{1/100}$ to $A_{1/10}$ ratio for A_{MAX} = 7 g at N = 525/947. Table A11 lists the percent difference values.

Table A10. Statistics for A_{MAX} = 7 g

N	Acceleration Statistics			
	A1/100 (g)	A1/10 (g)	A1/3 (g)	A1/100 / A1/10
100	4.776	2.952	2.025	1.618
200	4.821	3.157	2.154	1.527
300	4.550	3.070	2.155	1.482
400	4.913	3.077	2.185	1.597
500	5.221	3.133	2.189	1.667
600	5.540	3.261	2.235	1.699
700	5.440	3.282	2.247	1.658
800	5.379	3.281	2.234	1.639
900	5.303	3.229	2.227	1.642
947	5.355	3.257	2.245	1.644

Table A11. Percent Differences for A_{MAX} = 7 g

N	A1/100 (g)	% Diff from end value	A1/100 / A1/10	% Diff from end value
100	4.776	-10.807	1.618	-1.583
200	4.821	-9.971	1.527	-7.108
300	4.550	-15.029	1.482	-9.864
400	4.913	-8.246	1.597	-2.878
500	5.221	-2.497	1.667	1.380
600	5.540	3.449	1.699	3.316
700	5.440	1.595	1.658	0.838
800	5.379	0.440	1.639	-0.282
900	5.303	-0.975	1.642	-0.109
947	5.355	0.000	1.644	0.000